

Recoverable autonomous sonde (RECAS) for environmental exploration of Antarctic subglacial lakes: general concept

P.G. TALALAY,¹ V.S. ZAGORODNOV,^{1,2} A.N. MARKOV,¹ M.A. SYSOEV,¹ J. HONG¹

¹*Polar Research Center, Jilin University, Changchun City, China
E-mail: ptalalay@yahoo.com*

²*Byrd Polar Research Center, The Ohio State University, Columbus, OH, USA*

ABSTRACT. The proposed RECOVERABLE Autonomous Sonde (RECAS) will allow analysis and sampling of subglacial water while the subglacial lake remains isolated from the surface. The probe is equipped with two electrically heated melting tips, one on the bottom and one on the top of a cylindrical probe. When one of the tips is powered, the RECAS moves up or down similarly to a hot-point thermal electric drill. The electric power and signal cable is coiled inside the probe on an electric-motor-powered coil. When the lower tip is powered, the probe advances downwards by gravity. In order to move the probe up, power is applied to the upper heated tip and the coil motor pulls the cable, moving the probe upwards and melting the borehole above the probe. A conventional internal combustion engine electric generator on the glacier surface provides 9–10 kW of power to the RECAS via an umbilical cable stored in the probe. Electric power enables a penetration rate of 2.4–2.9 m h⁻¹, and thus 4–5 months will be required to reach a depth of 3500 m and return to the surface.

KEYWORDS: subglacial lakes

INTRODUCTION

A vast network of lakes, rivers and streams has been revealed thousands of meters beneath the Antarctic ice sheet. Sealed from the Earth's atmosphere for millions of years, the subglacial aquatic environment may provide unique information about microbial evolution and the Earth's climate in the past. The discovery of subglacial aquatic environments has opened up an entirely new area of science in a short period of time. By 2010, 387 subglacial lakes had been identified (Wright and Siegert, 2011); this number will increase as surveys improve spatial coverage. Estimates indicate that the total surface area of the subglacial lakes is nearly 10% of the ice sheet's base. The volume of Antarctic subglacial lakes alone exceeds 10 000 km³ (Dowdeswell and Siegert, 1999), with the largest being Vostok Subglacial Lake (6100 km³; Popov and others, 2011) and Lake 90° E (1800 km³; Bell and others, 2006).

In the past decades about a dozen deep drilling projects have been completed in Antarctica with the aim of reaching the ice-sheet bedrock and examining processes near the ice-sheet bed (Talalay, 2013); only four boreholes accessed the subglacial aquatic system. Subglacial water was reached for the first time in January 1968 at a depth of 2164 m, when the CRREL (US Army Cold Regions Research and Engineering Laboratory) electromechanical drill penetrated through the Antarctic ice sheet at Byrd Station (80°01' S, 119°32' W) (Ueda and Garfield, 1970). The thickness of the water layer was estimated to be <0.3 m. During an attempt to obtain a subglacial bedrock sample, the water entered the lower part of the borehole and mixed with the glycol solution used as drilling fluid. Freezing-out of the water created heavy slush in the lower 460 m of the hole. Within a few days, the slush became difficult to penetrate with the drill. No subglacial water samples were obtained at that time.

In summer 2006/07, within the framework of the European Project for Ice Coring in Antarctica (EPICA) at Kohnen station (75°00' S, 00°04' E), water entered the under-pressurized hole at a depth of 2774 m with a flow rate of >1 L min⁻¹

(Wilhelms, 2007). A sample of refrozen water was recovered by a special down-hole bailer. Upon reduction of the drilling fluid level, the bottom water rose to 173 m above the base. Subglacial water samples were polluted by the drilling fluid (a mixture of petroleum solvent Exxsol D40 and hydrochlorofluorocarbon HCFC-141b), and the decision was taken not to re-drill the refrozen water column because the ice formed would become contaminated.

In early February 2012 at Vostok station (78°28' S, 106°48' E), Russian researchers made contact with Vostok Subglacial Lake water at a depth of 3769.3 m (Talalay, 2012; Vasiliev and others, 2012). The drill was rescued from rapidly rising freezing lake water. The next drill deployment to the borehole was made in January 2013. The top of the frozen subglacial water was found at a depth of 3383 m (www.aari.nw.ru/news/text/2013/PA3100113.pdf [in Russian]), indicating that the water level in the borehole had risen by 386 m. The first core representing frozen lake water was opaque, porous and bright white ice. When the subglacial water first entered the borehole, it made contact and mixed with the drilling fluid (a mixture of aviation kerosene and hydrochlorofluorocarbon HCFC-141b), resulting in contamination of the subglacial water.

In December 2012, a UK consortium tried but failed to reach Ellsworth Subglacial Lake (78°58'34" S, 90°31'04" W) with a hot-water ice-drilling system (<http://www.ellsworth.org.uk/>); this research will be continued. In January 2013, the Whillans Ice Stream Subglacial Access Research Drilling (WISSARD) project succeeded in accessing Subglacial Lake Whillans (83°40' S, 145°00' W) with a similar hot-water drilling system (<http://www.wissard.org/multimedia/image-of-the-day/see-all>). Both water and sediment samples were collected from the lake and are being studied at the time of writing.

The main advantages of the exploration methodologies used for Ellsworth and Whillans subglacial lakes are that the equipment can provide samples of subglacial water and sediments with minimal contamination and that the lakes

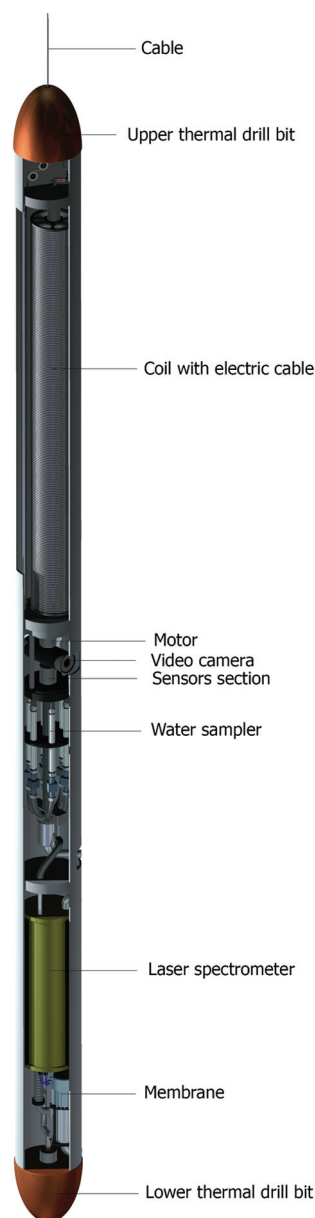


Fig. 1. Conceptual three-dimensional model of the RECAS (Talalay and others, 2013).

are accessed in a short time period. On the other hand, there are numerous disadvantages: (1) the equipment is expensive and heavy (>120 t); (2) the drilling technique requires a large amount of fuel (25 L m⁻¹); (3) the access hole cannot be kept open for more than a few days without reaming; and (4) the differential pressure while the lake is accessed is not predictable and, in the case of under-balanced drilling, could cause fluid blowout (as happened at Vostok station; Vasiliev and others, 2012).

The main function of the RECOVERABLE Autonomous Sonde (RECAS) is exploration of subglacial lakes with minimal chemical and microbial contamination (Talalay and others, 2013). The RECAS will have in situ analytical (embedded laser spectrometer) and sampling capabilities, and operate in the borehole isolated from the glacier surface and atmosphere. The RECAS design is based on the Philberth thermal probe, which was used to penetrate the Greenland ice sheet and measure temperatures while it descended to the glacier bottom (Philberth, 1976). The outstanding characteristic of this probe was that the wire for the

transmission of electrical power and signals was coiled inside the probe, and paid out when it was advancing and became fixed in the ice with frozen meltwater above it. In 1968 two Philberth thermal probes were launched at Jarl-Joset station, Greenland. The first probe reached a depth of 218 m and the second reached 1005 m below the ice-sheet surface before the main heater broke down. Unlike the non-recoverable Philberth thermal probe, the RECAS is designed to be recovered by using a cable recoiling mechanism. In this paper, the terms sonde and probe are synonymous and represent a sensor-instrumented drill used specifically for in situ measurements and sampling.

GENERAL CONCEPT AND EXPECTED PERFORMANCE OF THE RECAS

The RECAS is equipped with electrically powered melting tips located at the upper and lower ends of the apparatus (Fig. 1). The 150 mm diameter electrically heated melting tip (EHMT) produces a borehole; the diameter of the probe housing is 140 mm. The upper EHMT has a small central hole for the cable to slide into and out of the RECAS. To protect against refreezing, the exterior cylindrical surface of the sonde is heated by an element at an average power of ~0.45 W mm⁻¹ of housing length; for the 4 m long sonde the power required for side heating is estimated to be 1.8 kW.

About 10% of the melted water is pumped through sampling analytical devices and expelled to the water-filled borehole. The water inlet is located just above the lower EHMT. The gas dissolved in this water is separated in the membrane and analyzed by an embedded laser spectrometer. For this purpose, the OF-CEAS spectrometer system patented by the Interdisciplinary Laboratory of Physics (LIPhy), Grenoble, France, is being considered (Chappellaz and others, 2012). This spectrometer is based on the optical feedback cavity enhanced absorption spectroscopy technique. Methane and water vapor stable isotopes can be analyzed simultaneously with a resolution of 1‰ (for CH₄) and <1‰ (for δD) over ~1 min integration time.

Twelve 120 mL air-filled titanium sample bottles are installed in the middle of the RECAS. The bottle valves are actuated with magnetically coupled electric motors that open and close on demand. Samples are maintained at in situ hydrostatic pressure, enabling quantitative analysis of dissolved gases. The sonde is instrumented with an inclinometer, pressure gauge, thermometer, pH meter, sound velocity meter and water conductivity sensors. Video cameras and sonar provide additional information on the subglacial environment.

The power and signal cable coil is driven by a gear motor in the upper part of the probe. Two versions of the RECAS design are being considered: one with 1200 m of coiled cable and the second with a 4000 m long cable. To minimize the size of the cable, the power is supplied at 3000–4000 V d.c. and converted to the required voltage according to component specifications. The cable consists of two 0.2 mm² signal lines and two 2 mm² power lines. According to comparative analysis of alternative designs (Fig. 2), the smallest outer diameter of the cable (3.5–3.6 mm; Table 1) can be achieved with a coaxial cable design. The estimated length of the 1200 m coil is 1.3–1.5 m and of the 4000 m coil is 4.4–5.0 m. However, the effects of hydrostatic compression of the power cable insulation at significant depth have not been investigated and may pose a

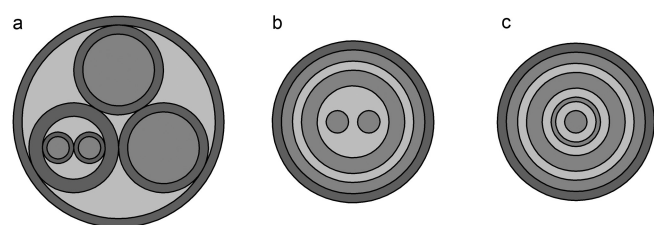


Fig. 2. Cable designs: (a) cable type; (b) coaxial type 1; (c) coaxial type 2.

high-voltage arc-over problem in a physical implementation of this concept.

All down-hole RECAS components will be sterilized using a combination of chemical wash, hydrogen peroxide vapor (HPV) and ultraviolet (UV) sterilization prior to deployment. A suggested field operation protocol is as follows (Fig. 3):

1. At the beginning of the summer, the RECAS and power and communication systems are installed on a dedicated area of the Antarctic ice sheet above a subglacial lake. The system is activated and the sonde starts to melt down to the ice-sheet bed.
2. The melted water is not recovered from the hole and it refreezes behind the sonde. The power and signal line is released from the coil inside the sonde. Part of the melted water is pumped into and through the sonde for analysis of methane and water stable isotopes. Penetration down to the subglacial reservoir at 1000 m depth is completed within 14–18 days, while accessing the deeply buried subglacial lake at 3500 m depth may take 50–60 days.
3. When the sonde enters the subglacial lake, it samples the water and examines water parameters: pressure, temperature, pH, sound velocity and conductivity.
4. When sampling and monitoring are complete, the coil motor is activated and the top EHMT is powered. Recovery of the sonde to the surface begins by spooling of the cable.
5. Finally, the sonde reaches the surface ready for servicing and moving to the next site by the research personnel.

Sounding of a relatively shallow subglacial lake can be conducted during the Antarctic summer; however, exploration of a deeply buried subglacial lake requires ~4–5 months. In the latter case, the research personnel leave the site after deployment and the sonde operates as a fully autonomous system. Coded data from the RECAS are transmitted to a computer on the surface and then automatically uploaded to webpages for inspection. Short message service (SMS) messages are sent automatically to a mobile phone to inform the operator that manual intervention is required. It is

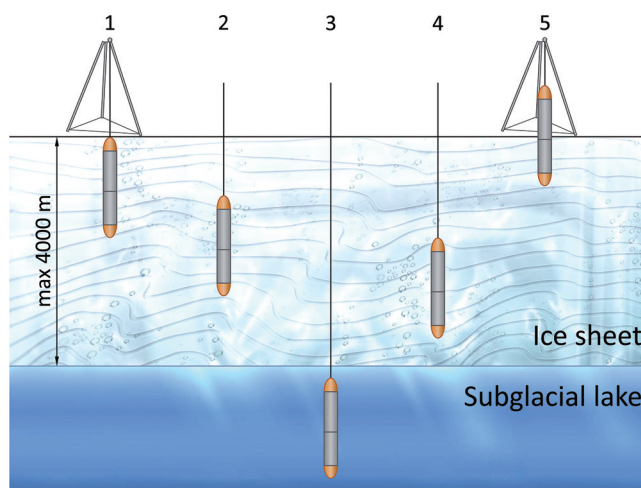


Fig. 3. RECAS subglacial access operation.

possible to establish a secure shell (SSH) link to the RECAS within a few minutes at any time.

SHAPE AND CLOSURE RATE OF THE RECAS BOREHOLE

During penetration into the ice, the RECAS forms a cylindrical borehole filled with meltwater. At distance h_f , heat carried with the water from the kerf is balanced by heat conduction to the ice surrounding the borehole (Fig. 4a). From that moment the borehole above h_f starts freezing. Depending on ice temperature, penetration rate and initial borehole radius, the RECAS probe could descend or be grasped by freezing ice.

Humphrey and Echelmeyer (1990) describe a calculation schema of borehole radius depending on initial ice temperature and time. In order to deal with temperature-dependent specific heat capacity and thermal conductivity of pure ice, empirical formulae published by Cuffey and Paterson (2010) were applied.

The estimated shape of a freezing borehole with initial radius 75 mm is shown in Figure 5a. Borehole radius is shown in two scales: (1) as a function of penetration time; and (2) as a function of distance above h_f that the RECAS travels during this time at a penetration rate of 2.5 m h^{-1} . Table 2 shows time and distance from h_f when the borehole radius reaches 70 mm, and time and distance from h_f when the borehole is completely frozen. The highest freezing rate occurs at the lowest temperature (Fig. 5a), and at chosen parameters the RECAS will be seized within 4 min and progress down to only ~0.2 m; at this temperature, complete closure of the borehole will occur in 50 min. Figure 5a demonstrates that the RECAS can pierce the ice freely at temperatures above -3°C (see also Fig. 4c), while penetration

Table 1. Main parameters of cable designs

Parameter	Cable type		Coaxial type 1		Coaxial type 2	
Outer diameter (mm)	4.7	3.6	3.5			
Cable length (km)	1.2	4	1.2	4	1.2	4
Coil length (m)	2.38	7.92	1.49	4.96	1.32	4.40

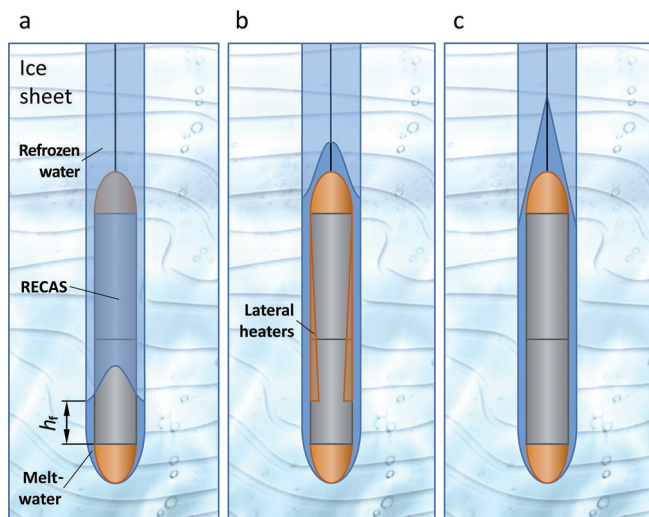


Fig. 4. Options for meltwater refreezing in the RECAS borehole: (a) at low temperatures without lateral heating; (b) at low temperatures with lateral heating; (c) in warm ice without lateral heating.

to ice at -60°C is possible either at a high penetration rate (360 m h^{-1}) or with large ($\sim 4.9\text{ m}$) initial borehole diameter. Both of these options require a large amount of power ($\sim 600\text{ kW}$). A more practical and economical solution is application of lateral heating to the device housing.

The lateral heater has to prevent refreezing of ice on the borehole wall during advance. The same relationship (Humphrey and Echelmeyer, 1990) was used to estimate the volume of ice that forms on the borehole wall. The power of the lateral heater is a product of ice volume and latent heat of melting ice. Figure 5b shows the power distribution along the RECAS housing required for the anti-freezing procedure.

Table 2. Borehole freezing parameters

Initial temperature t_i $^{\circ}\text{C}$	Borehole diameter decreases to diameter of the sonde		Borehole is completely frozen	
	Time hours	Distance from h_f m	Time hours	Distance from h_f m
-60	0.058	0.200	2.22	6.0
-50	0.088	0.221	3.08	8.0
-40	0.139	0.345	3.89	11.0
-30	0.214	0.531	5.83	15.3
-20	0.361	0.897	8.89	24.0
-10	0.694	1.725	19.4	50.1
-3	2.64	6.56	56.4	140.1
-2	3.89	9.66	88.9	221.0
-1	7.5	18.6	222.2	552.0

The maximum power of $\sim 1\text{ W mm}^{-1}$ of housing length has to be applied at the lower end of the housing just above h_f . It diminishes upward to 0.3 W mm^{-1} at a height of 4 m from h_f and increases to 0.72 W mm^{-1} in the next 1.5 m of housing. The power distribution on the RECAS surface is shown schematically in Figure 4b. Thus the power of a lateral heater required to keep a 4 m long borehole at a radius of 75 mm at -60°C is $\sim 1.8\text{ kW}$. At higher ice temperatures significantly less power is required. Measurements of the borehole diameter and freezing rate during penetration will allow optimization of power distribution between EHMTs and lateral housing heaters. During the RECAS return trip, the lateral heater power axial distribution has to be mirrored.

In our current estimates, one variable is still unknown. We consider measuring the heat that escapes from the melting

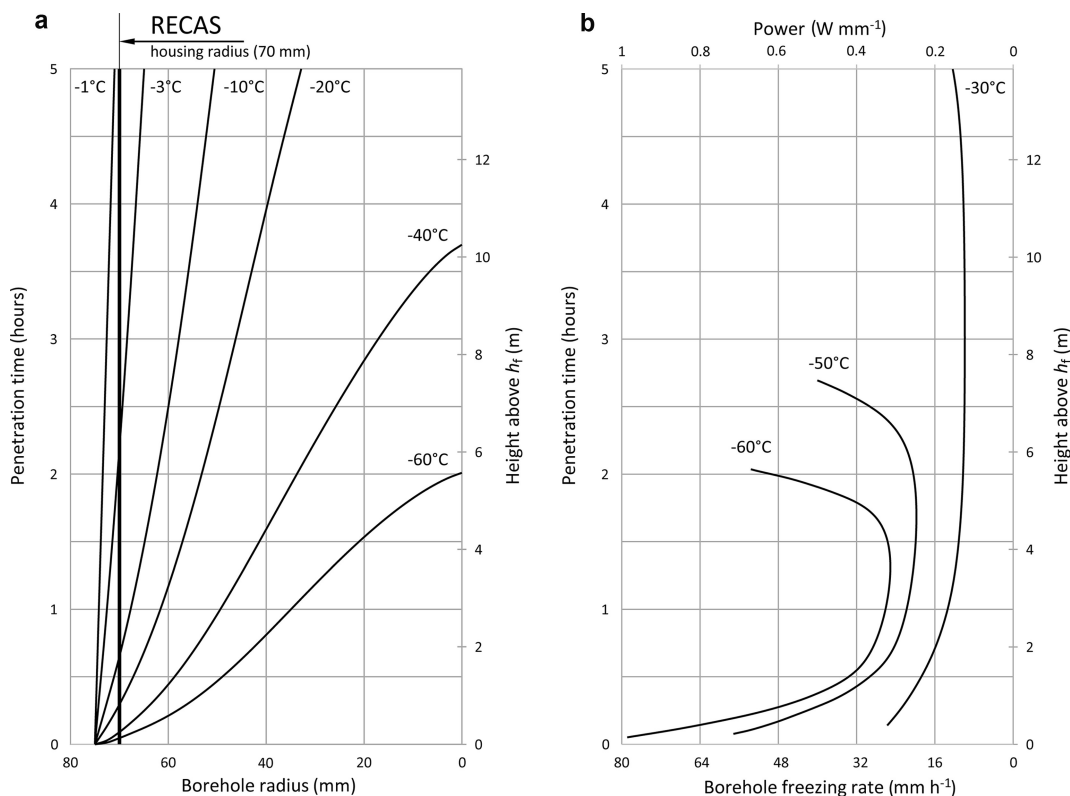


Fig. 5. Radius of freezing borehole (a) and power distribution along the RECAS housing required for the anti-freezing procedure (b).

kerf with water in experiments with prototype EHMTs. The more heat that escapes from the kerf, the less lateral heating will be needed; however, the more heat that is removed from the kerf, the lower the penetration. Slower penetration rate will increase borehole freezing time. Complete power optimization of the RECAS will be undertaken after experimental measurements of EHMT parameters, including power (heat) released from the kerf with meltwater.

PENETRATION TIP POWER

The EHMT is an important component of the probe as its lifespan and efficiency are related to the feasibility of the probe mission. The specific energy of the ice-drilling/melting process is

$$Q = Q_1 + Q_2 + Q_3 + Q_4 \tag{1}$$

where Q_1 is the specific energy required to raise the initial ice temperature from t_i to the melting point t_{mp} (kJ m^{-1}), Q_2 is the specific latent heat of melting ice (kJ m^{-1}), Q_3 is the specific lateral heat losses due to warming of the melted water from the melting point t_{mp} to the final temperature t_f (kJ m^{-1}) and Q_4 is the lateral conductive heat losses outside the borehole (kJ m^{-1}) (we assume this proportion of the heat losses as 2–5% of Q_1 ; Zotikov, 1986).

Then

$$Q_1 = c_i m_s (t_{mp} - t_i) \tag{2}$$

$$Q_2 = \lambda m_s \tag{3}$$

$$Q_3 = c_w m_s (t_f - t_{mp}) \tag{4}$$

where c_i is the specific heat capacity of ice ($\text{kJ kg}^{-1} \text{K}^{-1}$), m_s is the specific mass of ice (melted water) (kg m^{-1}), λ is the latent heat of melting ice (kJ kg^{-1}) and c_w is the specific heat capacity of water ($\text{kJ kg}^{-1} \text{K}^{-1}$).

The specific mass of ice can be found from

$$m_s = k_1 \frac{\pi D^2}{4} \rho_i \tag{5}$$

where k_1 is the coefficient accounting for the borehole enlargement during thermal drilling (1.03–1.05), D is the outer diameter of hot point m and ρ_i is the ice density (kg m^{-3}).

The power required for borehole melting is

$$N = \frac{Qv}{3600k_2} \tag{6}$$

where v is the expected rate of penetration (m h^{-1}) and k_2 is the coefficient of EHMT efficiency ($\sim 0.7\text{--}0.8$).

If the power of the EHMT is 5 kW, the expected speed of penetration in pure ice at a penetration efficiency of 0.75 is 2.4–2.9 m h^{-1} (Fig. 6). Values of the thermodynamic parameters of ice and water are (Cuffey and Paterson, 2010): $c_i = 2.05 \text{ kJ kg}^{-1} \text{K}^{-1}$, $\lambda = 334 \text{ kJ kg}^{-1}$, $c_w = 4.218 \text{ kJ kg}^{-1} \text{K}^{-1}$ and $\rho_i = 917 \text{ kg m}^{-3}$.

PENETRATION TIP SHAPE

Four conditions have to be achieved during design and fabrication of the EHMT: (1) durability, (2) penetration rate at definite efficiency, (3) even radial and angular heat flux distribution at the EHMT melting surface and (4) operation at high hydrostatic pressure. Over a dozen hot-point drills have been designed since the first device was used in the Jungfrau drilling project, European Alps, in 1948 (Gerrard and others,

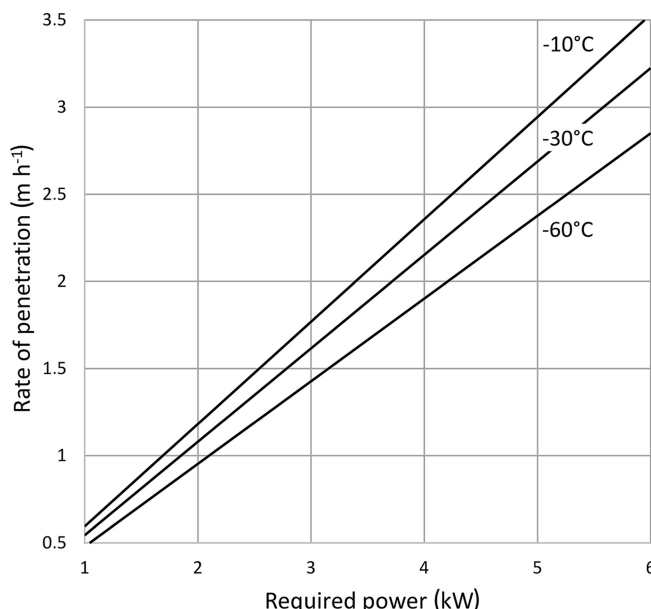


Fig. 6. Drilling/melting penetration rate in ice at different temperatures vs power.

1952). Among other advantages, a long cone-shaped EHMT with a parabolic end was found to be most favorable. The long cone shape makes it possible to move particles and pebbles aside while drilling in debris-containing basal ice (Sukhanov and others, 1974). In addition, the long cone tip provides better vertical stability during penetration. Recently, a new long cone hot-point tip was designed for, and operated during, the Ross Ice Shelf drilling operation in 2011 (Tyler and others, 2013). This shape of EHMT was chosen for thermal modeling.

Modeling of the temperature distribution inside the EHMT prototypes was carried out with steady-state heat transfer Autodesk Simulation Multiphysics. An isothermal work surface condition was simulated with introduction of the EHMT in the infinite water bath and free convection at the EHMT melting surface. Three types of heating elements were selected for prototype models: cartridge heater, ceramic tablet heater and coiled cable heater (Table 3).

Two major design tasks were achieved with the thermal models: (1) visualization of heat distribution in a long cone-shaped EHMT with three types of heaters, and concentration of heat output at the lower end of the EHMT; and (2) low interior temperature at electrical outlets. As the models show, the EHMTs equipped with cartridge heaters and ceramic heaters do not allow heat flux concentration at the lower end of the device (Fig. 7a and b). Realization of the required conditions is possible with coiled cable heaters mounted inside the grooves of a cone-shaped housing (Fig. 7c).

The durability of an electrical heater in the EHMT is secured by its operation at a lower than rated temperature. The option of multiple heating elements operated at a fraction of the EHMT's total power is possible in large-diameter (>80 mm) penetrating tips. Even radial and angular power distribution at temperatures lower than the rated operating temperature (650°C) can be obtained with a small diameter (1.6 mm) and long (>1500 mm) coiled cable heater mounted close to the melting surface of the tip. The cable heaters were tested in a high-pressure chamber at 800 bar for 96 hours and did not lose their containment.

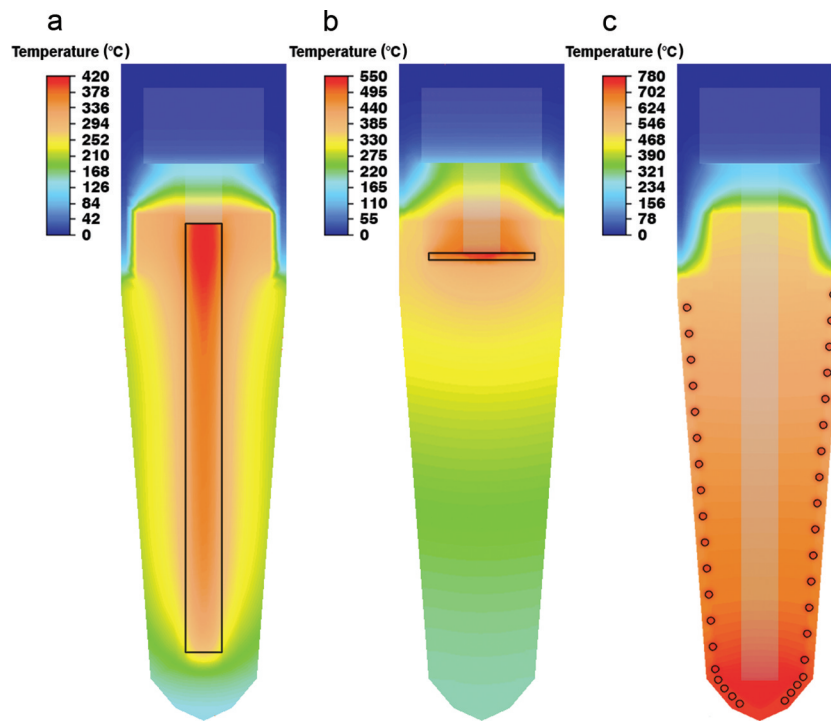




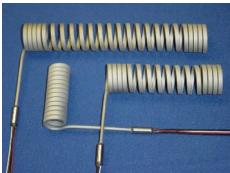
Fig. 7. Heat model of hot EHMt with different heating elements and equivalent power (2 kW): (a) cartridge heater; (b) ceramic tablet heater; (c) cable heater.

POWER SUPPLY CONSIDERATIONS

During the RECAS short version (with 1200 m of coiled cable) downward penetration, power consumption is summarized as follows: lower EHMt 5 kW; lateral heater 1.8 kW; coil motor 0.2 kW; sensors, down-hole computer,

spectrometer, etc. 1 kW; losses in cable 1.5 kW; total RECAS power requirement ~ 9.5 kW. During the return trip, the highest power consumption is summarized as: upper EHMt 5 kW; lateral heater 1.8 kW; coil motor 0.5 kW; sensors and down-hole computer 0.4 kW; losses in cable 1.5 kW; total power requirement ~ 9.2 kW.

Table 3. Main parameters of heating elements

Type	Power W mm^{-2}	Typical examples W mm^{-3}	
Cartridge heater	0.33	0.11	
Ceramic heater	0.69	0.53	
Cable heater	0.46*	1.55*	

*Submerged in water.

Power supply for exploration of shallow subglacial lakes down to 1000 m depth is not a problem as these operations can be undertaken during the summer with direct control. For penetration into deeply buried lakes, the RECAS power system has to operate continuously without service or refueling for ~ 5 months. In this case, we considered three types of power source: (1) solar power during summer with short-term power storage (batteries), (2) wind generator and (3) automatically controlled diesel engines during the dark winter months (Fig. 8).

In central Antarctica the sun shines for extended periods throughout the summer. Solar radiation vertical flux depends on latitude, and the highest possible flux is 350 W m^{-2} during December, the warmest month. Solar power can be converted into electricity by polycrystalline silicon cells with an efficiency of $\sim 25\%$ (Green and others, 2012). At low temperatures, power generation increases by 5% for every 10°C decrease in temperature compared with normal conditions (25°C). The average summer air temperature in central Antarctica is -30°C , resulting in an expected increase in power generation of 25%. To put this into a practical perspective, to generate 10 kW of electricity, $50\text{--}60 \text{ m}^2$ of photovoltaic panels have to be installed. Tests in central Antarctica showed that the ConergyC167P panel (1.2 m^2 , nominal power output of 167 W at 25°C) produced a maximum of $\sim 200 \text{ W}$ and an average of $\sim 2 \text{ kWh d}^{-1}$ when the sun was above the horizon for $> \sim 12$ hours (Lawrence and others, 2008). Solar power could be effective during summer, but at night and in winter an alternative power supply would have to be found.

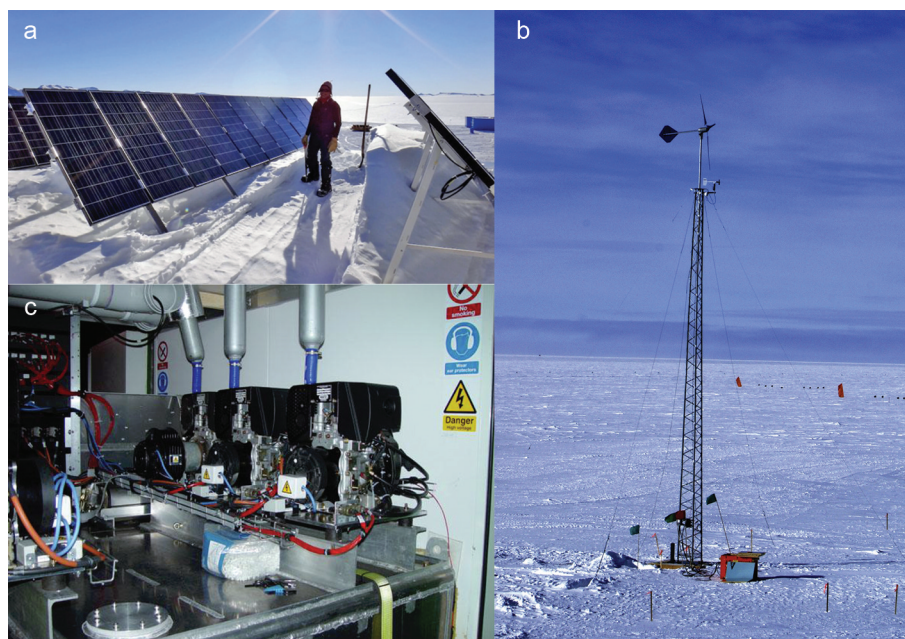


Fig. 8. RECAS power supply options: (a) solar panels (scientific base camp erected at the coast near Crown Bay (www.antarcticstation.org/news_press/news_detail/new_solar_panels_and_another_trip_to_the_coast/)); (b) autonomous wind generator (Raum model turbine installed at the South Pole in January 2011; Allison and others, 2012); (c) automatically controlled diesel generators (PLATO power system, Dome A; Hengst and others, 2008).

Autonomous wind turbine generators are a practical alternative renewable power source. The efficiency of the turbine depends on wind velocity. Tests of 1 kW wind generators (Raum, Hummer and Bergey types) showed that their power output depends on wind velocity raised to the power 2.8 (Allison and others, 2012). At a wind velocity of 5 m s^{-1} , the turbines generate $\sim 90 \text{ W}$. On the Antarctic plateau, katabatic winds are mild and this means low wind speed and low generator efficiency.

Therefore, solar and wind power are not practical for high-power load applications on the Antarctic plateau. The steady power output of diesel engine generators presents the best power supply option. No-live-operator Hatz 1B30 diesel generators have been used during winter by the PLATO (Plateau Observatory) Antarctic site testing observatory (Lawrence and others, 2008). The Hatz 1B30 is an air-cooled diesel engine with a maximum power output of $>1.5 \text{ kW}$ at the atmospheric pressure corresponding to the altitude of the Antarctic plateau. Operating the engines at only 2200 rpm enhances engine durability (nominal power at sea level is $5.4 \text{ kW}/3600 \text{ rpm}$).

To provide 10 kW of power, the more powerful Hatz 2L41C generator can be used. The standard output of this engine is 22 kW at sea level/3000 rpm. This type of engine has an extremely long service life that allows it to be operated reliably in remote areas or for applications without monitoring. The engines run on Jet-A1 fuel, and the estimated fuel consumption is $5\text{--}9 \text{ L h}^{-1}$, or $2.0\text{--}3.6 \text{ L m}^{-1}$ of borehole depth. A bank of large fuel and oil filters ensures stable performance, and the fuel tank has enough capacity for >5 months of continuous engine operation. Two engines alternate during continuous operation.

CONCLUSIONS

Because subglacial lakes and rivers have been isolated from the atmosphere for thousands or millions of years, they have

preserved unique microorganisms and contain sediments deposited in environments different from that of the present day. Currently, protocols for minimizing contamination and thermodynamic disturbance of subglacial aquatic environments have not been established, although a few initiatives to protect them have been formulated (e.g. Doran and Vincent, 2011). At present the main technical challenge for implemented and planned projects to access Antarctic subglacial lakes is the hydrostatic imbalance of subglacial reservoirs, which could result in the upwelling of water into the borehole, causing technical difficulties. Subglacial environment researchers have reached a consensus that as subglacial lakes are connected to the surface via a borehole, there is no assurance that modern microbiota will not get into the lakes.

The RECAS makes it possible to access subglacial water without connecting it to the modern atmosphere and without thermodynamic disturbance. The sonde is not only able to analyze and sample subglacial water, but also measure the geochemical composition of ice in situ. The RECAS can be used multiple times. In this paper we have presented a new technique that could reduce contamination compared with the technique of hot-water drilling.

Here we presented the concept of the RECAS based on conventional technologies and materials. The most complex part of the apparatus is the power transmission system. The size (diameter) of modern custom power and signal cable required is bulky, and therefore a coil occupies a large proportion of the length of the RECAS. In the near future, carbon nanotube cable will be available for practical applications (Zhao and others, 2011). Conductors made of carbon nanotube are expected to be significantly smaller, and thus allow a reduction in the length and/or diameter of the RECAS. In this case, the EHMT power could be increased by up to 50%, which will result in higher penetration rate, and the sounding could be completed much faster.

The RECAS probe and its field operation are relatively cheap: it is estimated to be 10–20 times less expensive than

penetration with a hot-water drilling system, while installation and operation requires four to five specialist staff. The first laboratory tests of the RECAS components are scheduled for 2014. Field tests of the RECAS in Antarctica are planned as soon as full financial and logistical support is obtained for the project.

ACKNOWLEDGEMENT

This paper presents the results of research conducted under 'The Recruitment Program of Global Experts' (also called 'The Thousand Talents Program') organized by the Central Coordination Committee on the Recruitment of Talents, China.

REFERENCES

- Allison P and 48 others (2012) Design and initial performance of the Askaryan Radio Array prototype EeV neutrino detector at the South Pole. *Astropart. Phys.*, **35**(7), 457–477 (doi: 10.1016/j.astropartphys.2011.11.010)
- Bell RE, Studinger M, Fahnestock MA and Shuman CA (2006) Tectonically controlled subglacial lakes on the flanks of the Gamburtsev Subglacial Mountains, East Antarctica. *Geophys. Res. Lett.*, **33**(2), L02504 (doi: 10.1029/2005GL025207)
- Chappellaz J, Alemany O, Romanini D and Kerstel E (2012) The IPICS 'oldest ice' challenge: a new technology to qualify potential sites. *Led i Sneg*, **4**(120), 57–64
- Cuffey KM and Paterson WSB (2010) *The physics of glaciers*, 4th edn. Butterworth-Heinemann, Oxford
- Doran PT and Vincent WF (2011) Environmental protection and stewardship of subglacial aquatic environments. In Siegert MJ, Kennicutt MCI and Bindschadler RA eds. *Antarctic subglacial aquatic environments*. (Geophysical Monograph Series 192) American Geophysical Union, Washington, DC, 149–157
- Dowdeswell JA and Siegert MJ (1999) The dimensions and topographic setting of Antarctic subglacial lakes and implications for large-scale water storage beneath continental ice sheets. *Geol. Soc. Am. Bull.*, **111**(2), 254–263 (doi: 10.1130/0016-7606(1999)111<0254:TDATSO>2.3.CO;2)
- Gerrard JAF, Perutz MF and Roch A (1952) Measurement of the velocity distribution along a vertical line through a glacier. *Proc. R. Soc. London, Ser. A*, **213**(1115), 546–558 (doi: 10.1098/rspa.1952.0144)
- Green MA, Emery K, Hishikawa Y, Warta W and Dunlop ED (2012) Solar cell efficiency tables (version 39). *Prog. Photovolt.: Res. Appl.*, **20**(1), 12–20 (doi: 10.1002/pip.2163)
- Hengst S and 6 others (2008) PLATO power: a robust low environmental impact power generation system for the Antarctic plateau. In Stepp LM and Gilmozzi R eds. *Proceedings of the SPIE Conference on Ground-based and Airborne Telescopes II, 27 August 2008*. (SPIE Volume 7012) Society of Photographic Instrumentation Engineers, Bellingham, WA
- Humphrey N and Echelmeyer K (1990) Hot-water drilling and bore-hole closure in cold ice. *J. Glaciol.*, **36**(124), 287–298 (doi: 10.3189/002214390793701354)
- Lawrence JS and 36 others (2008) The PLATO Antarctic site testing observatory. In Stepp LM and Gilmozzi R eds. *Proceedings of the SPIE Conference on Ground-based and Airborne Telescopes II, 27 August 2008*. (SPIE Volume 7012) Society of Photographic Instrumentation Engineers, Bellingham, WA
- Philberth K (1976) The thermal probe deep-drilling method by EGIG in 1968 at Station Jarl-Joset, central Greenland. In Spletstoeser JF ed. *Ice-core Drilling. Proceedings of the Symposium at University of Nebraska, 28–30 August 1974, Lincoln, NB, USA*. University of Nebraska Press, Lincoln, NB, 117–131
- Popov SV, Masolov VN and Lukin VV (2011) Ozero Vostok, Vostochnaya Antarktida: moshchnost' lednika, glubina ozero, podlednyy i korennoy rel'ef [Vostok Subglacial Lake, East Antarctica, ice thickness, lake depth, bedrock and ice base]. *Led i Sneg*, **1**(113), 25–35 [in Russian]
- Sukhanov LA, Morev VA and Zotikov IA (1974) Portativnyye termoelektrobury [Portable ice thermoelectric drills]. *Mater. Glytsiol. Issled./Data Glaciol. Stud.* **23**, 234–238 [in Russian with English summary]
- Talalay P (2012) Russian researchers reach subglacial Lake Vostok in Antarctica. *Adv. Polar Sci.*, **23**(3), 176–180 (doi: 10.3724/SPJ.1085.2012.00176)
- Talalay PG (2013) Subglacial till and bedrock drilling. *Cold Reg. Sci. Technol.*, **86**, 142–166 (doi: 10.1016/j.coldregions.2012.08.009)
- Talalay PG, Markov AN and Sysoev MA (2013) New frontiers of Antarctic subglacial lakes exploration. *Geogr. Environ. Sust.*, **6**(1), 14–28
- Tyler SW and 8 others (2013) Using distributed temperature sensors to monitor an Antarctic ice shelf and sub-ice-shelf cavity. *J. Glaciol.*, **59**(215), 583–591
- Ueda HT and Garfield DE (1970) Deep core drilling at Byrd Station, Antarctica. *IASH Publ.* **86** (Symposium at Hanover 1968 – *Antarctic Glaciological Exploration (ISAGE)*), 56–62
- Vasiliev NI, Lipenkov VY, Dmitriev AN, Podolyak AV and Zubkov VM (2012) Rezul'taty i osobennosti bureniya skvazhiny 5G i pervogo vskrytiya ozero Vostok [Results and characteristics of 5G hole drilling and the first tapping of Lake Vostok]. *Led i Sneg*, **4**(120), 12–20 [in Russian]
- Wilhelms F (2007) Sub-glacial penetration from an ice driller's and a biologist's perspective. *Geophys. Res. Abstr.*, **9**, 1607–7962/gra/EGU2007-A-09619
- Wright A and Siegert MJ (2011) The identification and physio-graphical setting of Antarctic subglacial lakes: an update based on recent discoveries. In Siegert MJ, Kennicutt MCI and Bindschadler RA eds. *Antarctic subglacial aquatic environments*. (Geophysical Monograph Series 192) American Geophysical Union, Washington, DC, 9–26
- Zhao Y, Wei J, Vajtai R, Ajayan PM and Barrera EV (2011) Iodine doped carbon nanotube cables exceeding specific electrical conductivity of metals. *Sci. Rep.*, **1** (doi: 10.1038/srep00083)
- Zotikov IA (1986) *Teplofizika lednikovykh pokrovov [The thermophysics of glaciers]*. (Glaciology and Quaternary Geology 2) D Reidel, Dordrecht